

CHARACTERISTICS OF CIRCULAR-CRESTED WEIR

By Amruthur S. Ramamurthy,¹ and Ngoc-Diep Vo²

ABSTRACT: The circular-crested weir is used for flow measurement and has wide applications in hydraulic engineering, where it serves as an overflow structure. It can be used to control the water level in farm ponds and reservoirs. The discharge coefficient of such a weir is obtained experimentally as a function of the dimensionless total head of the approaching flow. It is shown that changing the upstream slope does not alter the weir-discharge coefficient. However, increasing the downstream weir slope appears to increase the discharge coefficient. The weir crest pressure is determined as a function of the dimensionless head and its variation is related to the weir-discharge coefficient. The experimental data indicate that the circular-crested weir behaves like a sharp-crested weir, when the dimensionless total head is extremely large.

INTRODUCTION

The circular-crested weir is used for flow measurement and has wide applications in hydraulic engineering, where it serves as an overflow structure. It can be used to control the water level in farm ponds and reservoirs. The simplest form of such a weir consists of a circular crest of radius R set tangentially to an upstream face and perpendicular to the direction of flow (Fig. 1). The weir is commonly constructed with a downstream face having a slope β of 45° and has a high discharge coefficient C_D . Defining q as the discharge passing over a unit length of the weir crest, C_D can be related to q as follows:

$$q = \frac{2}{3} C_D \sqrt{2gH_1^3} \dots\dots\dots (1)$$

Here, g = acceleration due to gravity; and H_1 = total head of the approaching flow reckoned above the weir crest level. From direct measurement of the discharge passing over the weir model (Fig. 1), C_D can be evaluated using (1). According to Bos (1978), the crest pressure $(P/\gamma)_{cr}$ also denotes the minimum pressure $(P/\gamma)_{min}$ on the crest surface. Setting $Y_2 \approx 0.7 H_1$, and using the data of Escande and Sananes (1959), Bos (1978) related $(P/\gamma H_1)_{cr}$ with H_1/R . When the downstream slope of the weir $\beta = 45^\circ$ and $H_1/R < 10$, this relation can be rewritten as

$$\left(\frac{P}{\gamma H_1}\right)_{cr} \approx 0.71 - 0.44 \left(\frac{H_1}{R}\right) \dots\dots\dots (2)$$

For flow over circular-crested weirs for which $H_1/R \leq 1.0$, Matthew (1963) outlined a simple theory that clearly explains the influence of surface tension, viscosity, and the radius of curvature of the streamline on C_D . Cassidy (1965)

¹Prof., Civ. Engrg. Dept., Concordia Univ., 1455 de Maisonneuve West., Montreal, H3G 1M8, Canada.

²Grad. Student, Civ. Engrg. Dept., Concordia Univ., 1455 de Maisonneuve West, Montreal, H3G 1M8, Canada.

Note. Discussion open until February 1, 1994. To extend the closing date one month, a written request must be filed with the ASCE Manager of Journals. The manuscript for this technical note was submitted for review and possible publication on September 8, 1992. This technical note is part of the *Journal of Hydraulic Engineering*, Vol. 119, No. 9, September, 1993. ©ASCE, ISSN 0733-9429/93/0009-1055/\$1.00 + \$.15 per page. Technical note No. 4762.

$$C_D = \frac{q}{\frac{2}{3} \sqrt{2gH_1^3}} = \pi \left(\frac{H_1}{R} \right) \dots \dots \dots (3)$$

Here, $\pi ()$ denotes a function of H_1/R . Similarly, the normalized pressure head at the crest $(P/\gamma H_1)_{cr}$ can be expressed as

$$\left(\frac{P}{\gamma H_1} \right)_{cr} = \Phi \left(\frac{H_1}{R} \right) \dots \dots \dots (4)$$

Eqs. 3 and 4 represent the weir flow characteristics and $\Phi ()$ and $\pi ()$ denote different functions of H_1/R .

EXPERIMENTAL SETUP AND PROCEDURE

Machined plexiglass weir models were set in a smooth stainless steel flume (Fig. 1). The radii of the weir models were 0.0095 m, 0.0254 m, 0.0381 m, 0.0754 m, 0.1008 m, and 0.1516 m, and were true to the nearest 5×10^{-5} m. The test section was 0.254 m wide, 1.80 m high, and 2.50 m long. The side walls were equipped with transparent windows for flow visualization of separating flows, based on dye injection. Sufficient stilling arrangements were provided to obtain a smooth flow approaching the crest. To study the effects of weir slopes on C_D , tests were performed on weir models with combinations of upstream slopes α and downstream slopes β . The slopes were $\alpha = 90^\circ, 75^\circ$, and 60° in combination with downstream slopes $\beta = 75^\circ, 60^\circ$, and 45° . Tests were also conducted on sharp-crested weir models with sharp machined edge at the apex (1.5×10^{-4} m imperfection). These denoted the limiting case of a circular-crested weirs ($R/H_1 \rightarrow 0$). All models were equipped with sufficient pressure taps of diameter 0.5×10^{-3} m to record the pressure distribution along the model centerline. On the vertical weir face, pressure taps were spaced at every 0.05 m along the centerline. For models with $R \geq 0.0254$ m, taps were spaced at 5° intervals on the weir crest. The pressure head was recorded to the nearest 0.5×10^{-3} m. The water-surface profiles over the weir crest and the flow depth upstream of the weir were measured by means of point gages (Fig. 1) to the nearest 0.3×10^{-3} m. The flow rate was determined by measuring the flow depth over a standard 60° V-notch. The maximum error in the determination of the flow rate was estimated to be 3%.

RESULTS

Variation of C_D with H_1/R

Fig. 2 shows the experimentally determined relationship between C_D and H_1/R for circular-crested weirs for which $\alpha = 90^\circ$ and $\beta = 45^\circ$. For larger H_1/R , Bos (1978) used the data of Escande (1959) whose weir crest had a slot and showed that C_D attains an upper limiting value of 0.86 near $H_1/R = 5$ and remains unchanged for larger H_1/R (curve A, Fig. 2). The present data shows that C_D attains a maximum value of 0.87 as H_1/R is increased to 5.5 and then decreases with a further increase in H_1/R (curve B, Fig. 2). This discrepancy may be traced in part to the effect of the slot on C_D in the tests of Escande (1959). Fig. 3 denotes the expanded scale version of all the earlier data used by Bos (1978) to form the $C_D - H_1/R$ relation. It indicates that, even in the earlier studies, C_D increases gradually with an

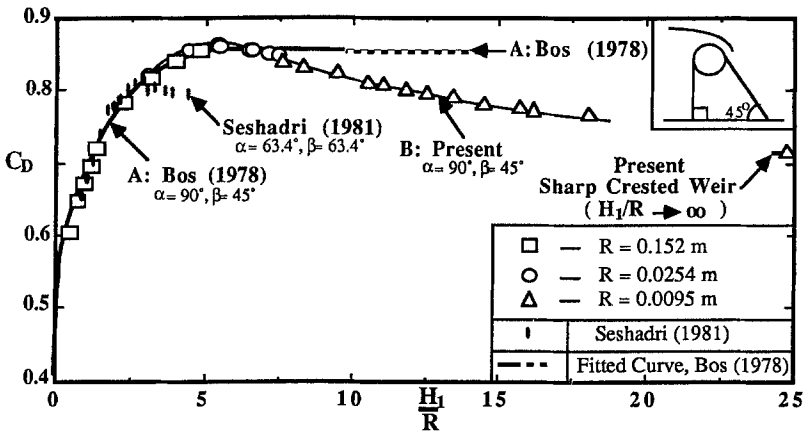


FIG. 2. Variation of C_D with H_1/R $0 < H_1/R \leq 25$

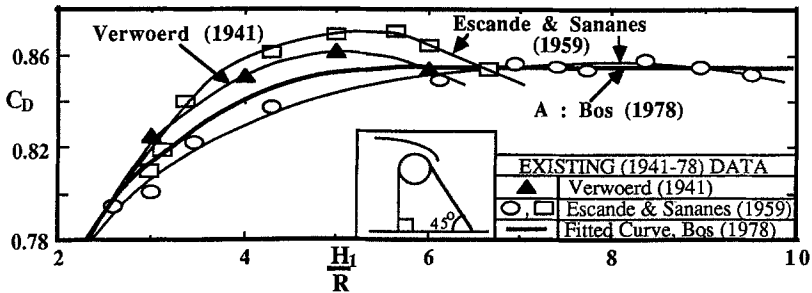


FIG. 3. Variation of C_D with H_1/R $2 \leq H_1/R \leq 10$

increase in H_1/R , attains a maximum value, and later decreases with a further increase in H_1/R . Fig. 2 also includes the results of more recent studies (Seshadri 1981), which confirm qualitatively the fact that C_D attains a maximum as H_1/R increases and later decreases with a further increase in H_1/R . For a weir with fixed R , both the subatmospheric pressure at the crest and C_D increase when H_1/R is increased, since the flow profile over the crest becomes steeper and more curved. However, when H_1/R is larger than five, the flow separates in the region BC (Fig. 1), and no further increase in C_D occurs. Further, at very large H_1/R , the value of C_D should drop and reach the value of C_D for sharp-crested weirs. The present experimental values of C_D for sharp-crested weir ($\alpha = 90^\circ, \beta = 45^\circ$) are also included in Fig. 2 to indicate that the circular-crested weirs behave like a sharp-crested weir at large H_1/R values ($H_1/R \rightarrow \infty$).

Crest Pressure

For circular-crested weirs with varying degrees of side slopes and $R \geq 0.0254$ m, the normalized crest pressure head $(P/\gamma H_1)_{cr}$ denoting the pressure at C (the highest point of the crest as shown in Fig. 1) is shown as a function of H_1/R in Fig. 4. It also shows that the dependence of $(P/\gamma H_1)_{cr}$ with H_1/R agree qualitatively with the approximate relation suggested by Bos (1978). He assumed $(P/\gamma H_1)_{cr} = (P/\gamma H_1)_{min}$. Since only the downstream

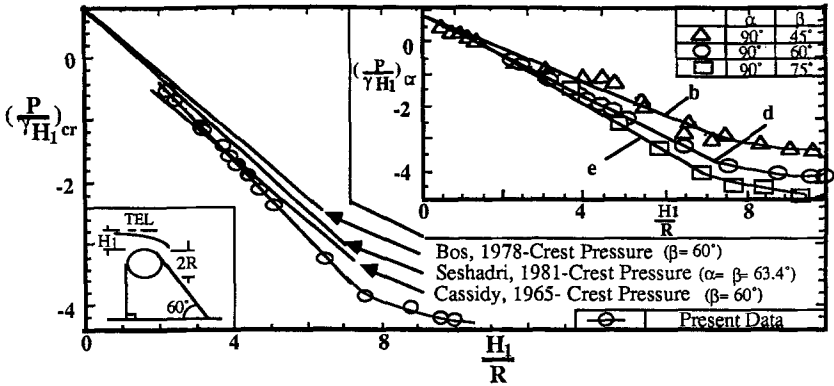


FIG. 4. Variation of $(P/\gamma H_1)_{cr}$ with H_1/R , Insert Shows Effect of β on $(P/\gamma H_1)_{cr}$

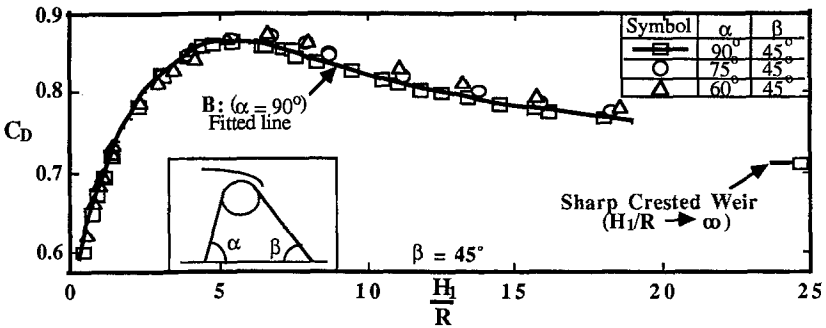


FIG. 5. Effect of Upstream Slope α on C_D - $(0 < H_1/R \leq 25)$

slope is influential in affecting C_D and $(P/\gamma H_1)_{cr}$, the data of Seshadri (1981) for symmetric weirs ($\alpha = \beta = 63.4^\circ$) are also included in Fig. 4 for comparison. His data compare well with the relation proposed by Bos (1978) and the present data ($\alpha = 90^\circ$ and $\beta = 60^\circ$). The present crest pressure data (Fig. 4) also agree well with the results of the ideal flow model of Cassidy (1965). The decrease in $(P/\gamma H_1)_{cr}$ due to an increase in H_1/R is arrested near $H_1/R = 8$. This corresponds to the value of H_1/R at which C_D is a maximum.

Effect of Upstream Weir Slope α on C_D

A gentle upstream slope contributes to the streamlining of the weir shape and tends to increase C_D . However, it adds to the upstream area over which flow occurs. This will tend to decrease C_D . The resulting effect on C_D is not significant in the range of tests covered (Fig. 5). Fig. 5 shows the variation of C_D with H_1/R for weirs with fixed downstream slope β and varying upstream slope α . The data indicate that the variation of α does not significantly change C_D at fixed H_1/R and fixed β . For instance, the deviation in C_D is at most 2% (Fig. 5) when α is changed from 90° to 60° in the entire range of tests ($0.45 \leq H_1/R \leq 18.5$) for the weir with a fixed downstream slope ($\beta = 45^\circ$). According to the test results, the changes in the upstream slope α did not significantly alter the value of C_D when the downstream

slope β was fixed at 60° and 75° . It may be added that these results compare favorably with the nearly constant upstream slope correction factor suggested by the Waterways Experiment Station (WES) for C_D of standard spillways (Bos 1978). For these spillways, α ranged from 45° to 90° , and p/H_1 was greater than 1.5.

Effect of Downstream Weir Slope β on C_D

For $0 < H_1/R \leq 3.5$ and $\alpha = 90^\circ$, curves E, D, and B of Fig. 6 indicate that C_D does not vary with the downstream slope ($45^\circ < \beta < 75^\circ$). However, for $H_1/R > 3.5$ and a fixed upstream slope $\alpha = 90^\circ$, a steeper downstream slope increases C_D . This peak value of C_D occurs at a higher H_1/R value, when β is increased gradually (Fig. 6). Escande and Sananes (1959) also observed that a steeper downstream slope improves the weir performance. It should, however, be noted that the flow at very high H_1/R is less stable when β values are very large ($\beta > 60^\circ$). The variation of C_D and H_1/R given by Cassidy (1965) for the ideal flow model of circular-crested weir is also shown in Fig. 6. The deviation between the results based on ideal flow and the present results can be traced in part to the presence of both the wall and crest boundary layers and the existence of flow separation in real flows. The data for two sharp-crested weirs that indicate the limiting case of the circular-crested weir ($H_1/R \rightarrow \infty$) are also included in Fig. 6 to indicate the value of C_D for large values of H_1/R . For $H_1/R > 3$, flow separation occurs ahead of C (Fig. 1), and the separating streamline (before reattaching downstream of C) will have a slightly steeper curvature when β is larger. Hence, at fixed H_1/R values, slightly lower $(P/\gamma H_1)_{cr}$ and higher C_D values are registered at larger β values.

Correlation between C_D and $(P/\gamma H_1)_{cr}$

The boundary layer thickness δ on the crest is thin ($\delta \ll H_1$), and the flow outside the boundary layer is irrotational. Hence, the crest pressures $(P/\gamma H_1)_{cr}$ are expected to be related directly with the maximum theoretical velocity $U_1 \approx \sqrt{2g(H_1 - (P/\gamma)_{cr})}$ at the edge of the boundary layer where the pressure is close to the crest pressure. Lower crest pressures are associated with higher values of U_1 , and thus improve the weir performance in terms of C_D . The insert of Fig. 4 shows the variation of the crest pressure

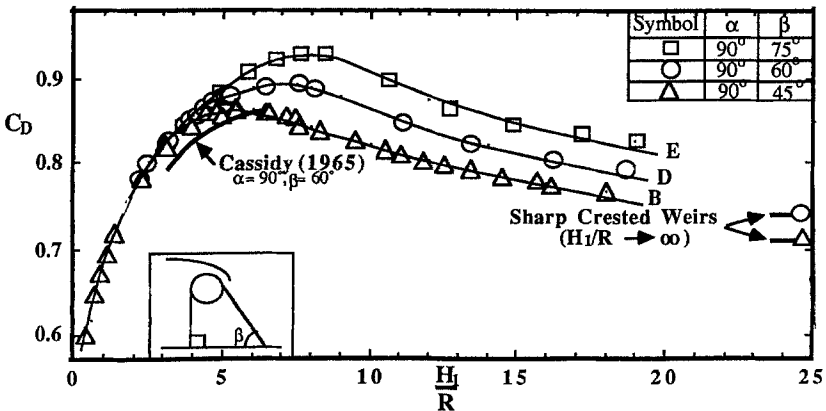


FIG. 6. Effect of Downstream Slope β on C_D - ($0 < H_1/R \leq 25$)

for circular-crested weirs with various slopes. Here, the curves b, d, and e should be viewed with the corresponding curves, B, D, and E of Fig. 6. Fig. 6 and the insert in Fig. 4 show that up to H_1/R close to 2.5, $(P/\gamma H_1)_{cr}$ and C_D are essentially the same for all the models tested. Further, they also indicate that for $H_1/R > 2.5$, variations in C_D values are correlated with the crest suction pressures attained at various H_1/R and β values.

CONCLUSIONS

For the commonly used circular-crested weir with $\alpha = 90^\circ$ and $\beta = 45^\circ$, the variation of C_D with H_1/R in the lower range $0 < H_1/R \leq 5.5$ generally agrees very well with the results of previous studies. However, for $H_1/R > 5.5$, C_D decreases, and for very large values of H_1/R , the C_D value approaches the C_D value for sharp-crested weirs with the same side slopes. A somewhat similar trend in the $C_D - H_1/R$ relationship is noticed for weirs with other upstream and downstream slopes.

For a fixed downstream slope, the effect of upstream weir slope on C_D is marginal. For a fixed upstream weir slope, for $3 < H_1/R$, C_D increases when the downstream slope is increased.

The variations in C_D are directly correlated with the crest suction pressures $(P/\gamma H_1)_{cr}$ for all the weir types tested.

APPENDIX I. REFERENCES

- Bos, M. G. (1978). "Discharge measurement structures." *Publ. 20*, Int. Inst. for Land Reclamation and Improvement, Wageningen, (ILRI), The Netherlands.
- Cassidy, J. J. (1965). "Irrotational flow over spillways of finite height." *J. Engrg. Mech. Div.*, ASCE, 91(6), 155–173.
- Escande, L., and Sananes, F. (1959). "Étude des seuils déversants à fente aspiratrice (Weirs with suction slots)." *La Houille Blanche*, 14(Special B), 892–902.
- Matthew, G. D. (1963). "On the influence of curvature, surface tension and viscosity on flow over round-crested weirs." *Proc. of the Inst. of CE*, 25, 511–524.
- Seshadri, S. (1981). "Flow characteristics of hydrofoil weirs, hydrofoil topped weirs and streamlined triangular profile weirs," PhD thesis, Indian Institute of Science, Bangalore, 012, Karnataka State, India.
- Sinniger, R., and Hager, W. H. (1985). "Flood control by gated spillways." *Commission Internationale des Grands barrages, 15^e Congrès des barrages*, Int. Commission on Large Dams, Q.59(R.9) 121–149.
- Verwoerd, A. L. (1941). "Calcul du débit de déversoirs dénoyés et noyés à crête arrondie." *L'Ingénieur des Indes Néerlandaises*, 8, 65–78.

APPENDIX II. NOTATION

The following symbols are used in this paper:

- C_D = coefficient of discharge;
 g = acceleration due to gravity;
 H = total head reckoned above crest level;
 h = piezometric head, flow depth above crest level;
 P = pressure;
 p = weir height;
 q = discharge per unit width;
 R = radius of circular crest;
TEL = total energy line;

- U_1 = maximum velocity at crest, ideal flow ($U_1 = \sqrt{2g(H_1 - (P/\gamma)_{cr})}$);
 x = x -direction, horizontal distance;
 Y = total flow depth;
 y = y -direction, vertical distance, depth from bed;
 α = upstream slope angle;
 β = downstream slope angle;
 γ = specific weight of water;
 δ = boundary layer thickness; and
 $\pi, \Phi()$ = function of.

Subscripts

- 1 = approach section 1, index;
 2 = downstream section 2, index;
 cr = at weir crest; and
 min = at minimum value.